# Ca2+ ENTRY PATHWAYS IN MOUSE SPINAL MOTOR NEURONS IN CULTURE FOLLOWING *IN VITRO* EXPOSURE TO METHYLMERCURY

**Gunasekaran Ramanathan** and **William D. Atchison**
Department of Pharmacology and Toxicology, Michigan State University, East Lansing, MI 48824

## Abstract

Methylmercury (MeHg) is a widespread environmental toxicant which affects the central nervous system. Among neurons reportedly affected in cases of mercury poisoning are motor neurons; however, direct cellular effects of MeHg on motor neurons have not been reported. Ratiometric fluorescence imaging and fura-2, were used to examine effects of MeHg on $Ca^{2+}$ homeostasis in mouse spinal motor neuron primary cultures. *In vitro* MeHg exposure at concentrations (0.1 μM-2μM/30–40 min) which affect other neurons in culture differentially, induced a biphasic rise in fura-2 fluorescence ratio indicating increased $[Ca^{2+}]_i$. Times-to-onset of these effects were inversely correlated with MeHg concentration. TPEN (20 μM), a non-$Ca^{2+}$, divalent cation chelator, reduced the amplitude of the first phase increase induced by MeHg, indicating that both $Ca^{2+}$ and non-$Ca^{2+}$ divalent cations contribute to the MeHg-induced effect. Contributions of intra- and extracellular $Ca^{2+}$ were compared using $Ca^{2+}_i$ -free solutions containing 20 μM EGTA. The second phase resulted from $Ca^{2+}_e$ influx. Among possible pathways contributing to $Ca^{2+}$ influx, the excitatory amino acid (EAA) receptor blockers MK-801 (15 μM), and AP-5 (100μM)- both NMDA receptor-operated ion channel blockers, CNQX (20μM), a non-NMDA receptor blocker, and the voltage-dependent $Ca^{2+}$ channel blockers nifedipine (1 μM) and ω-conotoxin-GVIA (1 μM) all significantly delayed the development of increased $Ca^{2+}$ caused by MeHg. Tetrodotoxin (TTX, 1 μM) did not alter the MeHg-induced effects. Thus, MeHg alters $[Ca^{2+}]_i$ in mouse spinal motor neurons through excitatory amino acid receptor-mediated pathways, and nifedipine and ω-conotoxin-GVIA-sensitive pathways.

### Keywords

Intracellular $Ca^{2+}$ regulation; motor neurons; fura-2 fluorescence; divalent cations; excitatory amino acid receptors

## INTRODUCTION

Environmental toxicants including heavy metals and pesticides have been postulated to be risk factors for age-related neurodegeneration (Chancellor et al., 1993; Armon, 2003).

Address all correspondence including reprint requests to: Dr. William D. Atchison, Michigan State University, Department of Pharmacology and Toxicology, B-331 Life Sciences Bldg, East Lansing, MI 48824-1317, Phone: 517-353-4947, Fax: 517-432-1341, atchiso1@msu.edu.

However, for the most part this concept remains untested. Methylmercury (MeHg) is a potent environmental neurotoxicant, to which humans are exposed primarily through consumption of contaminated sea food and marine mammals (Clarkson, 2002; Clarkson and Magos, 2006). MeHg exposure causes alterations in $Ca^{2+}$ homeostasis (Levesque et al. 1992), including elevations in intracellular $Ca^{2+}$ (Limke et al., 2003), decreased mitochondrial viability (Franco et al., 2007), increased reactive oxygen species formation (Usuki et al., 2001; Shanker et al., 2003; Mori et al., 2007) and oxidative stress (Daré et al., 2000), all of which can contribute to neurodegeneration. Several brain regions, including the visual cortex (Nagashima, 1997) and granule layers of the cerebellum (Hunter and Russell, 1954; Leyshon-Sørland et al., 1994), are particularly vulnerable to MeHg toxicity. Perinatal exposure to MeHg unquestionably impairs neuronal development, especially to the cerebellum and calcarine cortex. Postdevelopmental exposure can also cause neurological impairment. However, the extent to which MeHg exposure can hasten senescence-related neurodegeneration is unknown.

One neurodegenerative disease for which there is likely to be an environmental link is amyotrophic lateral sclerosis (ALS), also known as motor neuron disease. Approximately 90% of all cases of ALS lack association with a known genetic linkage and are referred to as sporadic ALS (SALS). No specific environmental neurotoxicants have been linked definitively to ALS, but one group of agents that has been proposed as risk factors in ALS are neurotoxic metals including $Pb^{2+}$ and $Hg^{2+}$ (Mitchell, 1987; Praline, 2007; Oh et al., 2007; Kamel et al., 2002; Vanacore et al., 1995; Johnson and Atchison, 2009; Kamel et al., 2008; Callaghan et al., 2011).

Motor neuron dysfunction is not typically considered to be a primary target of mercurials, however, there are observations from both human and animal literature that support this possibility. MeHg exposure reversibly decreased both rat motor nerve conduction velocity and tail flick response (Chuu et al., 2007). Chronic treatment of rodents with MeHg induces degeneration of spinal motor neurons (Su et al., 1998). Exposure of mice to Hg vapor caused a marked increase in avidin binding to the perikarya of spinal motor neurons - an indicator of oxidative damage to DNA (Pamphlett et al., 1998). After a single dose of $HgCl_2$, mercury deposits were localized in spinal motor neurons and brainstem motor nuclei (Arvidson, 1992). Thus exposure to mercury by various routes can 1) cause accumulation of the metal in spinal motor neurons, and 2) can lead to their toxicity.

Little is known about mechanisms by which MeHg could affect motor neuron function. However, in ALS, motor neurons exhibit vulnerability to $Ca^{2+}$ -mediated excitotoxicity (Van den Bosch et al., 2006, 2011; Grosskreutz et al., 2010), an effect commonly associated with MeHg exposure (Atchison and Hare, 1994; Limke et al., 2004). Recent data from our lab demonstrates that chronic MeHg exposure of the SOD1G93A mouse ALS model hastens the onset of ALS phenotype in a $Ca^{2+}$ -dependent manner (Johnson et al., 2011). Thus, as a prelude to examining chronic effects of MeHg on motor neuron $Ca^{2+}$ homeostasis directly, the present study was undertaken to identify early onset targets of MeHg. Consequently, this report focuses on the possible effect of MeHg-induced alterations in $Ca^{2+}$ homeostasis in spinal motor neurons in culture.

## MATERIALS AND METHODS

### Chemicals and solutions

Spinal motor neuron cell culture supplies, including Dulbeccos modified eagle medium (DMEM) and fetal bovine serum, were obtained from Gibco BRL (Grand Island, NY). Deoxyribonuclease I (DNase) was purchased from Worthington Biochemicals (Freehold, NJ). Trypsin, cytosine β arabinofuranoside, glutamine, penicillin, streptomycin, ethylene

diamine tetra-acetic acid (EDTA), brain derived neurotrophic factor (BDNF), ciliary neurotrophic factor (CNTF), N-methyl D-aspartic acid (NMDA), kainic acid, 5-aminophosphonovaleric acid (AP-5), 6-cyano-7-nitroquinoxaline-2,3-dione sodium salt (CNQX), tetrakis (2-pyridylmethyl) ethylethylenediamine (TPEN), ethyl glycol, $N$, $N$, $N'$, $N'$-tetraacetic acid (EGTA), tetrodotoxin (TTX), ω-conotoxin-(ω-CTx-GVIA), primary antibody against glial fibrillary acidic protein (GFAP), goat secondary antibody FITC-(fluorescein isothiocyanate), and poly D- lysine, were all purchased from Sigma Aldrich (St. Louis, MO). Rabbit polyclonal antibody against choline acetyl transferase (ChAT) was purchased from Chemicon International Inc. Methylmercuric chloride (MeHg) was purchased from ICN Biomedicals Inc. (Aurora, OH). 5-Methyl-10, 11-dihydro-5H-dibenzo[a,d]cyclohepten-5,10-imine hydrogen maleate (MK-801) was obtained from Ascent Scientific Co (Princeton, NJ).

## Experimental solutions used

Depending upon the specific experiment, variations of physiological saline were used to maintain consistency with published literature methods. HEPES-buffered saline (HBS) was used for isolation of spinal motor neurons and fura-2 microfluorimetry. It contained (mM): 160 NaCl, 5.4 KCl, 1.8 $CaCl_2$, 0.8 $MgSO_4$, 20 $d$-glucose, and 20 HEPES (free acid) (pH 7.3 at room temperature of 23– 25°C). The KCl depolarization buffer contained the following: (mM) 105.4 NaCl, 40 KCl, 1.8 $CaCl_2$, 0.8 $MgSO_4$, 20 $d$-glucose and 20 HEPES (free acid) (pH 7.3). The $Ca^{2+}$ -free HBS lacked $CaCl_2$ but had the addition of 20 μM EGTA. NaCl was increased appropriately to maintain osmolarity.

MeHg was made up as a stock solution in deionized water (10 mM) and diluted to the needed working concentrations just prior to use. All pharmacological mediators used in this study were dissolved in either HBS, absolute ethyl alcohol or DMSO to a maximum final solvent concentration of 0.01% [v/v]. Appropriate controls were included for any additional solvents used.

Pathways associated with entry of extracellular $Ca^{2+}$ into motor neurons were examined pharmacologically. Both voltage- and ligand-gated channels were examined. Specific antagonists of voltage gated sodium (TTX), and calcium (nifedipine and ω-conotoxin GVIA) channels, as well as excitatory amino acid (EAA) receptors (CNQX- AMPA receptors, MK801 and AP-5 -NMDA receptors) were used to examine the pathways by which MeHg-induced increases in $[Ca^{2+}]_i$ occurred. For each blocker, preliminary experiments were conducted using a range of at least three concentrations (data not shown). The final inhibitor concentration was selected based on it's ability either to delay a MeHg response, in which case an intermediate concentration was chosen, or inability to do so, in which case the maximum concentration was selected. In each instance, the concentration selected was consistent with that used in previous experiments and cells in culture (Hare et al., 1993; Marty and Atchison, 1997, 1998).

## Isolation and culturing of mice spinal motor neurons

All animal procedures were approved by the Institutional Animal Use and Care Committee at Michigan State University and were in accordance with NIH guidelines. In brief, following euthanasia, spinal cords were removed from newborn mice (4 –6 days old) and quickly immersed in HBS. After removal of the dorsal root ganglia, the tissue was minced in 1–3 mm blocks and immersed in 3.5 ml of HBS with 0.01 mg DNAse with 200 units/ml streptomycin, 200 units/mL penicillin and 0.1% EDTA (w/v). After 3 min, the tissue was dissociated using HBS with 1ml 10X trypsin. It was further dissociated by mechanical trituration for 10–15 min. Following centrifugation (EBA-21, Hettich, Beverly, MA) at 4000 RPM ($1780\times g$) for 4 min, the cells were plated at a density of 100 cells/$cm^2$ on 25 mm

round glass coverslips in a petri dish, in DMEM medium supplemented with 5 μM cytosine arabinoside to inhibit glial cell proliferation; 20 mM glutamine, 100 units penicillin, 200 units/ml streptomycin, and 10% fetal calf serum, 1ng/ml BDNF, 10 ng/ml CNTF and 0.1 ml DNase (1mg/ml stock) were added at this time. The medium was changed with muscle extract 3.3% (v/v) (Schulz et al., 1990) every 2 days, and measurements were performed after 5–7 days when the cells were clearly distinguishable as neurons having at least two neurites, one of which was the length of the cell body (Fig 1A). Motor neurons were identified on the basis of their soma size (50 μm), which is larger than other spinal cord neurons. However, we initially verified motor neuron identity by immunolabeling with choline acetyl-transferase (ChAT) and SMI32 (See Figure 1B, 1C). The former is the enzyme catalyzing formation of acetylcholine, the endogenous transmitter at vertebrate neuromuscular junctions. The latter, is an antibody (Wong et al., 1993), that stains an epitope on cell bodies of a nonphosphorylated form of 200 kD Heavy neurofilament (NP-NF) found in high concentration in Aα motor neurons in the ventral horn of the spinal cord (Tsang *et al.*, 2000).

## Preparation of muscle extract

The muscle extract was prepared using a modification of the method of Schulz et al., (1990). Four g of gastrocnemius muscle (from new born to one day old mouse pups) were homogenized in 12 ml of 50 mM, Tris -HCl buffer (pH 7.2). This was centrifuged at $100,000 \times g$ for 1 h at 4°C. The supernatant was aliquoted and stored at −80°C. Working solution was prepared by diluting the stock solution and filtering through a sterile 0.22 μm polyvinyl difluoride (PVDF) membrane (Millipore, Billerica, MA). Skeletal muscle provides a target-derived trophic support for the survival of motor neurons. Hence, we added skeletal muscle to the culture medium to increase the survival and differentiation of motor neurons under control conditions.

## Immunocytochemistry for ChAT

Eight day old (DIV) spinal motor neuron cultures were fixed with 4% (v/v) paraformaldehyde in 0.1 mM phosphate buffer saline (PBS- pH 7.4). It consisted of (mM): 137 NaCl, 2.7, KCl, 1.4 $NaH_2PO_4$, and 4.3 $NaH_2PO_4$. Fixed cultures were incubated for 10 min each in 0.1% (v/v) Triton X-100 with 0.1 mM PBS, and then methanol containing 1% (v/v) $H_2O_2$. Nonspecific staining was blocked by incubating the cells with 20% (v/v) normal goat serum in PBS, containing 0.1% Triton X-100 for one h, rinsing 3X, and incubating the fixed cells overnight at 4°C with rabbit polyclonal anti-ChAT (1:1000). Subsequently, the fixed cultures were rinsed 3X with 0.1 mM PBS followed by 2 hrs incubation in the dark with FITC-conjugated goat anti-rabbit IgG antibody (Sigma: 1:200). They were finally rinsed 3X with 0.1 mM PBS and mounted in mounting medium. Immunofluorescent images were acquired using a Nikon Eclipse TE 2000-U fluorescent microscope (Nikon Optics, Tokyo, Japan).

## Immunocytochemistry for SMI-32

Spinal motor neuron cultures were fixed with 4% (v/v) paraformaldehyde for 30 min at room temperature, washed 3X with 0.05% (v/v) Tris (pH 7.6) and then incubated for 20 min in the blocking solution (3% normal goat serum in Tris with 0.3% Triton X-100). Fixed cultures were subsequently incubated in primary antibody SMI-32 mouse monoclonal (1:1000 dilutions with 0.05 M Tris (pH 7.4, Houser et al., 1984) containing 1% normal goat serum) for 48 h at 4°C. Sodium azide (2%) was added to the primary antibody solution for overnight incubations and fluorescence visualized using secondary antibody TRITC (Tetramethyl rhodamine iso-thiocyanate) goat anti- mouse IgG 1:100 in 0.05 M Tris (pH 7.4) containing 1% normal goat serum. Fluorescence images were acquired using a Nikon fluorescent microscope (Nikon Optics, Tokyo, Japan).

## Measurement of fura-2 fluorescence changes

To track changes in $[Ca^{2+}]_i$, fura-2 fluorescence was measured using microfluorometric imaging. Digital images were obtained using a Nikon Diaphot microscope coupled to an Ionoptix system (Ionoptix, Milton, MA) with an open microincubator (Harvard Apparatus, Holliston, MA). Cells were loaded for 40–45 min in the dark at 37°C with 2 – 3 μM fura-2 acetoxymethylester, (depending on size and density of cells) in HBS. After loading, pre-warmed HBS (pH 7.3) was used for cell perfusion.

For each experiment, changes in emitted fluorescence (505 nm) at excitation wavelengths of 340 and 380 nm were monitored simultaneously in the soma of multiple motor neurons (3–7 cells). The same microscopic field was used to avoid cell selection bias. Data from these cells were averaged to provide a mean time-to-onset for that dish ($n=1$). The fluorescence ratio (340 nM/380 nM) indicated the approximate $[Ca^{2+}]_i$. However, previous studies in our laboratory reported that MeHg exposure induced fluorescence increases that may not fully depend on $Ca^{2+}$, but instead have a contribution of other divalent cations, most likely $Zn^{2+}$ (Hare et al., 1993; Denny et al., 1993; Denny and Atchison, 1994; Edwards et al., 2005). Thus values are only reported here as changes in fluorescence ratio. The potential contribution of non-$Ca^{2+}$ divalent cations to MeHg-induced changes in fura fluorescence was examined by exposing spinal motor neurons to MeHg in the presence of the non-$Ca^{2+}$ divalent cation chelator TPEN (20 μM) (Fukuyama et al., 2011). The relative contribution of intracellular and extracellular sources of $Ca^{2+}$ to the MeHg-induced elevation in fura-2 fluorescence ratio was examined using $Ca^{2+}$ -free solutions containing 20 μM EGTA.

After exposure to MeHg, motor neurons exhibit a shift in fura- 2 fluorescence ratio consistent with an increase of $[Ca^{2+}]_i$. The time course of development of these fluorescence changes was very consistent within each cell isolate but dependent on the MeHg concentration. For each fura2-measurement 7 different isolations were made (for each culture isolation 5–6 pups were used).

To identify the various $Ca^{2+}$ entry pathways as possible targets contributing to $Ca^{2+}$ influx following MeHg exposure, we used blockers for various ion channels. These included voltage-gated $Ca^{2+}$ and $Na^+$ channels as well as ionotrophic glutamate receptors. Exposure of motor neurons to MeHg in the presence or absence of inhibitors was done consecutively on cells from the same isolate on the same experimental day (separate dishes were used for each inhibitor). All ion channel blockers were preapplied for 7 min prior to exposure to MeHg. Cells were loaded with fura-2, and then exposed to 0.1–1.0 μM MeHg with or without channel blockers. After loading, all experiments began with a 10 min wash with HBS (to establish baseline fluorescence), followed by 1–1.5 min exposure to 40 mM $K^+$ solution; only cells which showed a reversible increase in $Ca^{2+}$ following the $K^+$ exposure were considered to be viable and with sufficient $Ca^{2+}$ buffering capacity to be suitable for the experiment. The $K^+$ solution was replaced for 5 min with HBS, and then cells were first exposed to excitatory amino acid (EAA) receptor blockers: NMDA receptor antagonists AP-5 or MK801 and the AMPA receptor antagonist CNQX. Experiments were carried out in $Mg^{2+}$ -free perfusion buffer in order to remove the $Mg^{2+}$ -induced block of the NMDA-activated channel (Nowak et al., 1984). CNQX and AP-5 were each prepared as 10 mM stock solutions in distilled $H_2O$ prior to dilutions. MK-801 was prepared as a 2 mM stock solution in dimethyl sulfoxide (DMSO) 0.1%. Corresponding control experiments verified that solvent (i.e., DMSO or absolute ethyl alcohol)-exposed spinal motor neurons did not undergo elevations in basal fluorescence ratio (results not shown).

Second, cells were exposed to L- and N-type voltage-gated $Ca^{2+}$ channel antagonists: 1 μM nifedipine and 1μM ω-CTx GVIA, respectively. Nifedipine was diluted from 10 mM stock solutions prepared in absolute ethyl alcohol; ω-CTx GVIA was diluted from 5 mM stock

solutions prepared in distilled $H_2O$. Experiments utilizing nifedipine were all done in a darkened room and nifedipine solutions were stored in brown bottles covered with aluminum foil to prevent photodegradation. Subsequently, cultures were exposed to the voltage-gated sodium channel blocker tetrodotoxin (TTX, 1 μM).

The effects of the channel blockers on MeHg-stimulated increase in fluorescence were examined by comparing the times to onset of the two phases of increased fluorescence in the presence and absence of the channel blockers. In this way, each cell served as its own control. Thus, percentage of activity remaining in the presence of the inhibitor was determined as: $F_I/F_O \times 100$, where $F_I$ = stimulated fluorescence ratio-baseline fluorescence ratio in the presence of an inhibitor; and $F_O$ = stimulated fluorescence ratio-baseline fluorescence ratio in the absence of an inhibitor. A single control group was used for comparison with each of the chemical inhibitors in each separate group- i.e. $Ca^{2+}$ channel blockers, EAA antagonists and TTX.

### Statistical Analysis

For time-to-onset of both phases (MeHg exposure in the absence and presence of blockers), the values are presented as mean ± SEM. One way analysis of variance followed by Tukeys *post-hoc* test were used to compare the time courses of action of MeHg alone to that of MeHg with channel blocker. *P*<0.05 was considered to be statistically significant. A Kruskal-Wallis nonparametric ANOVA was used to examine the relationship between MeHg concentration and time to onset of the first and second phase increase in fura-2 fluorescence (Fig. 3).

## RESULTS

Prior to treatment with MeHg, all cells were exposed to 40 mM KCl for 1.5 min. This ensured adequate loading of fura-2, as well as functionality of the cell. KCl caused a rapid and transient increase in fura-2 fluorescence (Fig. 2). Transience reflects adequate rebuffering capacity of the cells to changes in $[Ca^{2+}]_i$. Once the fluorescence ratio returned to basal levels, cells were allowed to re-equilibrate prior to exposure to MeHg (0.1–1μM). Only cells exhibiting such a response to KCl were used in subsequent experiments.

Exposure of cultures of spinal motor neurons to 0.1 to 1μM MeHg caused a temporally distinct biphasic increase in the ratio of fura-2 fluorescence (Fig. 2). These characteristic shifts in fura-2 fluorescence were observed in all cells exposed to MeHg. There is a significant difference between time-to-onset response at 0.1 μM MeHg and higher concentrations (p < 0.05), indicating that the time-to-onset of both phases was inversely related to MeHg concentration (Fig. 3). The magnitude of the fluorescence changes did not appear to be concentration-dependent, as all concentrations of MeHg tested induced comparably large elevations in fura-2 fluorescence ratio followed by fura-2 loss. This latter effect was presumably due to cell damage (results not shown).

Previous studies in our laboratory using NG108-15 and cerebellar granule cells showed that the first phase elevation in fluorescence is due to an increase in cytosolic $Ca^{2+}$ released from intracellular stores; the second phase is due to an influx of extracellular $Ca^{2+}$ (Hare et al., 1993; Limke and Atchison, 2002). Thus the next experiment was to characterize the contributions of intracellular and extracellular $Ca^{2+}$ to the increases in fura-2 fluorescence in motor neuron cultures. Cells were exposed to 0.5 μM MeHg in $Ca^{2+}$ -free buffer. A representative tracing of these data is shown in Figure 4 in $Ca^{2+}$ -deficient solutions, MeHg still caused a first phase increase in fluorescence. Though not shown, for the composite of the group, the time-to-onset of the first phase in normal or $Ca^{2+}$ -free buffers did not differ. However, in the presence of EGTA, the second phase was always absent. Thus, the source

of $Ca^{2+}$ contributing to fluorescence changes during the first phase is primarily intracellular, whereas the second phase is due to influx of extracellular $Ca^{2+}$. The motor neuron response to MeHg is qualitatively similar to that of other cells in culture (Hare et al., 1993; Marty and Atchison, 1997), or rat brain synaptosomes (Denny et al., 1993).

To examine whether the elevation of fluorescence observed during the first phase was due exclusively to $Ca^{2+}$, cells were exposed to MeHg with TPEN (20 μM), a chelator which does not bind substantially to fura-2, $Ca^{2+}$ or MeHg (Arslan et al., 1985; Komulainen and Bondy, 1987; Hare et al., 1993). When TPEN was added, there was a significant decline in the fluorescence ratio during elevation in the first phase (Fig. 5, Table 1) indicating that other divalent cations also contribute to the fluorescence response to MeHg (Denny and Atchison, 1994). However, the second phase did ensue in the presence of TPEN. Thus, TPEN-sensitive fluorescence presumably resulted from release of internally bound metal.

The level of fluorescence change in the second phase is considerably greater than that of the first, and in other neuron types it's solely due to extracellular $Ca^{2+}$ influx (Hare et al., 1993; Marty and Atchison, 1997). When the extracellular $Ca^{2+}$ was removed by EGTA, we observed that there is a significant absence of the second phase indicating that this phase is due primarily to influx of $Ca^{2+}$ (Fig. 4, Table 1). Experiments were consequently undertaken to determine the route(s) of $Ca^{2+}$ influx. A variety of $Ca^{2+}$ entry pathways exist in spinal motor neurons including EAA receptor-operated channels (Choi, 1988) and voltage-dependent $Ca^{2+}$ channels (Bean, 1989; Randall and Tsien, 1995), any of which could contribute to the MeHg response.

### Effect of EAA inhibitors

There are numerous reports correlating activation of EAA receptor channels with $Ca^{2+}$ -mediated excitotoxicity in spinal motor neurons (Delfs et al., 1997; Feldman et al., 1997; Urushitani et al., 2001). To test whether glutamate receptor-mediated pathways contributed to the MeHg-induced increase in $[Ca^{2+}]_i$, we exposed cells to various EAA inhibitors prior to MeHg in an attempt to block or delay the MeHg-induced increase in fura-2 fluorescence ratio. To inhibit the NMDA receptor-operated pathway, 100 μM AP-5 (Muller et al., 1988), or 15 μM MK-801 (Foster and Wong, 1987; Davies et al., 1988), were used in $Mg^{2+}$ -free buffer. AP-5 or MK-801 delayed the onset of both phases significantly ($p < 0.05$) compared to cells exposed to MeHg alone (Fig. 6A and 6B).

The potential role of AMPA/kainate receptor channels was tested by use of 20 μM CNQX. It too significantly ($p < 0.05$) altered the time-to-onset of MeHg-induced changes in fura-2 fluorescence (Fig. 6A and 6B). These data support the hypothesis that EAA receptor-operated channels contribute to the MeHg-induced increase in fura-2 fluorescence ratio during the second phase.

### Effect of nifedipine (Nif) and ω-conotoxin (ω-Ctx-GVIA)

The potential role of high voltage-activated $Ca^{2+}$ channels in the second phase was tested using Nif (μM), and ω-CTx GVIA (1 μM), which block L- and N-type $Ca^{2+}$ channels, respectively. Both channel antagonists significantly ($p < 0.05$) delayed the time-to-onset of the second, but not the first $Ca^{2+}$ phases (Fig. 7).

### TTX does not affect the response to MeHg

In certain preparations, MeHg appears to interact either directly or indirectly with voltage-gated $Na^+$ channels (Traxinger and Atchison, 1987; Shafer and Atchison; 1992, Hare and Atchison, 1995b). Consequently we examined in spinal motor neurons whether voltage-gated $Na^+$ channels contributed to the change in $[Ca^{2+}]_i$ induced by MeHg- perhaps due to

extracellular membrane depolarization. Spinal motor neurons were exposed to 0.5 μM MeHg alone or in the presence of (1 μM) TTX, a $Na^+$ channel blocker (Moore et al., 1967; Hille, 1970). The onset of neither phase was affected by TTX ($p$ >0.05, Fig. 8). Therefore, $Na^+$ channels did not contribute to the effect of MeHg on $[Ca^{2+}]_i$ in spinal motor neurons. These data differ from previous findings in the NG108-15 cells, in which TTX slowed the onset of the changes in $Ca^{2+}$ induced by MeHg (Hare and Atchison, 1995b).

## DISCUSSION

We studied the possible route(s) responsible for $Ca^{2+}$ entry of spinal motor neurons in culture in response to acute MeHg exposure using single cell microfluorimetry and fura-2 fluorescence. We selected this model as a prelude to future studies in our laboratory in which spinal cord cultures will be exposed chronically to MeHg. It is essential to know what the effects of acute exposure to the metal are, prior to beginning chronic exposure.

In many respects, the acute effects of MeHg on spinal motor neurons mimic those on other cells in culture. However, there are some notable distinctions. The principal findings of these studies are that spinal motor neurons exposed to MeHg show a biphasic rise in fura-2 fluorescence ratio, the first phase, which is EGTA-insensitive, is due to release of $Ca^{2+}$ from intracellular stores. The second phase, which is blocked by EGTA treatment, is due to $Ca^{2+}$ influx from extracellular sources, as also shown in other studies (Hare et al., 1993; Marty and Atchison, 1997). We also observed that MeHg exposure increased intracellular concentrations of a non- $Ca^{2+}$ cation such as $Zn^{2+}$, $Fe^{2+}$ or $Mn^{2+}$. $Ca^{2+}$ influx during the second phase was delayed significantly following EAA receptor antagonists and L- and N-type channel blockers -Nif and ω-CTx GVIA respectively, prior to and during MeHg exposure. In contrast, TTX exposure had no effect on elevations of fluorescence ratio stimulated by MeHg. With *in vitro* exposure of spinal motor neurons, there is an inverse correlation between the concentration of MeHg used and the time-to-onset of elevations in fluorescence ratio. The reasons for this latency with MeHg remain enigmatic. MeHg binds to protein sulfhydryl groups (Hughes, 1957; Rabenstein, 1978); thus there are numerous binding sites with which MeHg may interact. Despite that, MeHg exhibits uncanny selectivity for certain neuronal cell types during poisoning episodes. Furthermore, it acts with high potency at some membrane protein targets. The latency period may occur at lower concentrations because a longer period is required for sufficient amount of MeHg to reach its binding sites.

Both intracellular stores, and $Ca^{2+}$ -permeable channels contribute to changes in $[Ca^{2+}]_i$ caused by MeHg in primary cultures of mouse spinal cord motor neurons. In this regard, the effects of MeHg on spinal motor neurons are consonant with those of transformed and primary neurons (Hare et al., 1993; Marty and Atchison, 1997; Limke et al., 2003). In these cell types, the first phase elevation in fluorescence ratio was due to release of $Ca^{2+}$ from an inositol 1, 4, 5-trisphosphate (IP3)-sensitive pool (Hare and Atchison, 1995a; Limke et al., 2003), whereas the second phase required $Ca^{2+}$ influx (Hare et al., 1993) and though specific intracellular stores were not identified in the present study, the overall pattern of effects of MeHg on motor neurons is similar to that of other neurons.

Spinal motor neurons are quite sensitive to MeHg-induced fluorescence changes; their sensitivity is on par with that of the highly MeHg-susceptible cerebellar granule cells (Marty and Atchison, 1997; Edwards et al., 2005). Exposure to 0.1 μM MeHg induced elevations in fluorescence ratio in spinal motor neurons, whereas effective MeHg concentrations in the Purkinje cells and two transformed cell lines were ~10X higher. This implies that like granule cells, spinal motor neurons contain sensitive targets to MeHg. This difference may also reflect the lack of $Ca^{2+}$ binding proteins in spinal motor neurons.

In rat brain synaptosomes and NG108-15 cells, MeHg-induced elevation in the first phase involves not only $Ca^{2+}$, but also other cations such as $Zn^{2+}$, $Fe^{2+}$, and $Mn^{2+}$ (Denny and Atchison, 1994). Similarly, in this study, TPEN (a non-$Ca^{2+}$ cation chelator, Fukuyama et al., 2011) suppressed the first phase fluorescence, demonstrating a contribution of other divalents in addition to $Ca^{2+}$ to the changes induced by MeHg (Aizenman et al; 2010). The second phase is not associated with the non-$Ca^{2+}$ divalent cation, but is completely dependent on influx of $Ca^{2+}$. It was not observed in the presence of extracellular EGTA but was present in 1.8 mM extracellular $Ca^{2+}$ and TPEN. This demonstrates that $Ca^{2+}$ was indeed the cation responsible for the large changes in fura-2 fluorescence during the second phase, and the release of intracellular divalent cations is not necessary to induce the increase in $Ca^{2+}$.

If $Ca^{2+}$ is involved in MeHg-induced cell damage and death, the route of influx of $Ca^{2+}$ into cells during the 2nd phase following MeHg exposure is extremely important. Spinal motor neurons have numerous pathways for $Ca^{2+}$ influx, including EAA and nicotinic cholinergic receptor-activated channels (Westenbroek et al., 1995; Temkin et al., 1997), voltage-dependent $Ca^{2+}$ channels, and reversal of the $Na^{2+}/Ca^{2+}$ exchanger. The sheer multiplicity of $Ca^{2+}$ entry routes in spinal motor neurons may contribute to its heightened sensitivity to MeHg. As such, a major component of this study was devoted to assessing the contribution of various pathways of $Ca^{2+}$ entry to MeHg-induced disruption of cytoplasmic $Ca^{2+}$ (Limke et al., 2004). We evaluated this by testing the ability of antagonists for EAA receptors, voltage-gated $Ca^{2+}$ and $Na^{2+}$ channels to delay the onset of fura-2 fluorescence increases. A reduction in the overall level of MeHg-induced increase was not expected based on the results of other studies, which demonstrate a more or less "all or none" type of response of cells to MeHg-induced changes in $[Ca^{2+}]_i$ (Hare et al., 1993, Hare and Atchison, 1995a,b; Marty and Atchison, 1997; Edwards et al., 2005).

Because of numerous reports linking EAA receptor-operated channel activation with spinal motor neuron death (Lei et al., 1992), we first tested the contribution of EAA receptors to MeHg-induced response. Blocking both NMDA and AMPA receptors delayed the action of MeHg. An obvious question is where the stimulus for EAA receptor activation arises in the absence of exogenous agonist application. The most likely source is endogenous glutamate released into the medium in the presence of MeHg, a potent action demonstrated in isolated brain slices (Yuan and Atchison, 2007). This glutamate could then auto-activate adjacent motor neurons (Schramm et al., 1990; Delfs et al.,1997; Feldman et al., 1997; Urushitani et al., 2001). However, spinal motor neurons are cholinergic, not glutamatergic, so other cell types in the mixed culture must have been the source of this putative glutamate. Because the cultures were astrocyte deficient, the EAAT2 transporter, which is astrocyte based, would by and large be absent. This would allow any glutamate that was released into the medium by actions of MeHg on sensory neurons to linger, thereby increasing its likeliness of activating the ionotrophic glutamate receptors on the motor neurons.

In examining the role of voltage-gated $Ca^{2+}$ channels in the MeHg-induced changes in fura-2 fluorescence in spinal motor neurons *in vitro,* experimental results were consistent with previous studies; only the second phase was delayed with ω-CTx- GVIA (Randall and Tsien, 1995) or Nif. ω-CTx-GVIA is a relatively selective and potent inhibitor of N-type $Ca^{2+}$ channels ($Ca_V$ 2.2), including those in turtle spinal motor neurons (Aguilar et al., 2004), whereas Nif blocks L-type $Ca^{2+}$ channels in dorsal root ganglia (Fox et al., 1978). Thus at least these two types of voltage-gated $Ca^{2+}$ channels contribute to the increase in fura-2 fluorescence during the second phase.

One difference between the response to MeHg of spinal motor neurons and some other neurons (NG-108-15, for example) is the role of voltage-gated $Na^+$ channels. TTX did not

alter the time-to-onset of MeHg-induced increase in fluorescence ratio in motor neurons (Fig. 8). This is surprising, because at rat neuromuscular junctions, the synapses made by motor neurons on muscle, $Na^+$ channels <u>do</u> participate in the effects of MeHg (Atchison, 1987; Traxinger and Atchison, 1987; Shafer and Atchison, 1992). $Na^+$ channels in squid axon are also sensitive to block by MeHg (Shrivastav et al., 1976). However Komulainen and Bondy (1987) found no effect of 5μM TTX on the MeHg-induced changes in fluorescence in rat brain synaptosomes. Thus the contributory role of $Na^+$ channels to the actions of MeHg appears to be cell type dependent.

In summary, MeHg alters $Ca^{2+}$ homeostasis in mouse spinal motor neurons through EAA receptors, and nifedipine and ω-conotoxin-GVIA-sensitive pathways, suggesting that NMDA and non-NMDA receptors, as well as L- and N- type $Ca^{2+}$ channels, contribute to either the mode of action or entry of MeHg. Spinal motor neurons, though responding generally similarly to MeHg as do other neurons, exhibit very high sensitivity to MeHg. Whether or not this reflects a predisposition of these cells to MeHg-induced neurotoxicity *in vivo* remains to be seen.

## Acknowledgments

## Abbreviations used

| | |
|---|---|
| **ALS** | Amyotrophic lateral sclerosis |
| **AMPA** | α-amino-3-hydroxy-5-methylisoxazole-4-propionate |
| **ANOVA** | analysis of variance |
| **BDNF** | brain derived neurotrophic factor |
| **$[Ca^{2+}]_i$** | intracellular $Ca^{2+}$ concentration |
| **ChAT** | choline acetyltransferase |
| **CNQX** | 6-cyano-7-nitroquinoxaline-2,3-dione |
| **CNTF** | ciliary neurotrophic factor |
| **DIV** | day *in vitro* |
| **DMEM** | dulbecco's modified Eagle medium |
| **DMSO** | dimethyl sulfoxide |
| **EAA** | excitatory amino acid |
| **EGTA** | ethylene glycol tetraacetic acid |
| **HEPES** | *N*- [2- hydroxyethyl]piperazine-*N′*-[2-ethanesulfonic acid] |
| **FITC** | fluoroscein isothiocyanate |
| **HBS** | HEPES-buffered saline solution |
| **$IP_3$** | inositol 1, 4, 5-trisphosphate |
| **MeHg** | methylmercury |
| **NMDA** | *N*-methyl-D-aspartate |
| **ω-CTx-GVIA** | ω-conotoxin GVIA |

| PC12 | pheochromocytoma cells |
|---|---|
| **SOD1** | superoxide dismutase 1 |
| **TPEN** | tetrakis (2-pyridylmethyl) ethylethylenediamine *N*, *N*, *N′*, *N′*-tetraacetic acid |
| **TRITC** | tetramethyl rhodamine isothiocyanate |
| **TTX** | tetrodotoxin |
| **VGCC** | voltage-gated $Ca^{2+}$ channels |

## References

Aguilar J, Escobedo L, Bautista W, Felix R, Delgado-Lezama R. N- and P/Q-type $Ca^{2+}$ channels regulate synaptic efficacy between spinal dorsolateral funiculus terminals and motoneurons. Biochem Biophys Res Commun. 2004; 317:551–7. [PubMed: 15063793]

Aizenman E, McCord MC, Saadi RA, Hartnett KA, He K. Complex role of zinc in methamphetamine toxicity in vitro. Neuroscience. 2010; 171:31–9. [PubMed: 20801194]

Armon C. An evidence-based medicine approach to the evaluation of the role of exogenous risk factors in sporadic amyotrophic lateral sclerosis. Neuroepidemiology. 2003; 22:217–28. [PubMed: 12792141]

Arslan P, Di-Virgilio F, Beltrame M, Tsien RY, Pozzan T. Cytosolic $Ca^{2+}$ homeostasis in Ehrlich and Yoshida carcinomas. A new, membrane-permeant chelator of heavy metals reveals that these ascites tumor cell lines have normal cytosolic free $Ca^{2+}$ J Biol Chem. 1985; 260:2719–27. [PubMed: 3919006]

Arvidson B. Inorganic mercury is transported from muscular nerve terminals to spinal and brainstem motoneurons. Muscle Nerve. 1992; 15:1089–94. [PubMed: 1383815]

Atchison WD. Effects of activation of sodium and calcium entry on spontaneous release of acetylcholine induced by methylmercury. J Pharmacol Exp Ther. 1987; 241:131–9. [PubMed: 2437285]

Atchison WD, Hare MF. Mechanisms of methylmercury-induced neurotoxicity. FASEB J. 1994; 8:622–9. [PubMed: 7516300]

Bean BP. Classes of calcium channels in vertebrate cells. Annu Rev Physiol. 1989; 51:367–84. [PubMed: 2540697]

Callaghan B, Feldman D, Gruis K, Feldman E. The association of exposure to lead, mercury, and selenium and the development of amyotrophic lateral sclerosis and the epigenetic implications. Neurodegener Dis. 2011; 8(1–2):1–8. Epub 2010 Aug 4. Review. [PubMed: 20689252]

Chancellor AM, Slattery JM, Fraser H, Warlow CP. Risk factors for motor neuron disease: a case-control study based on patients from the Scottish Motor Neuron Disease Register. J Neurol Neurosurg Psychiatry. 1993; 56:1200–6. [PubMed: 8229031]

Choi DW. Glutamate neurotoxicity and diseases of the nervous system. Neuron. 1988; 1:623–34. [PubMed: 2908446]

Chuu JJ, Liu SH, Lin-Shiau SY. Differential neurotoxic effects of methylmercury and mercuric sulfide in rats. Toxicol Lett. 2007; 169:109–20. [PubMed: 17292570]

Clarkson TW. The three modern faces of mercury. Environ Health Perspect. 2002; 110:11–23. [PubMed: 11834460]

Clarkson TW, Magos L. The toxicology of mercury and its chemical compounds. Crit Rev Toxicol. 2006; 36:609–62. [PubMed: 16973445]

Daré E, Götz ME, Zhivotovsky B, Manzo L, Ceccatelli S. Antioxidants J811 and 17β-estradiol protect cerebellar granule cells from methylmercury-induced apoptotic cell death. J Neurosci Res. 2000; 62:557–65. [PubMed: 11070499]

Davies SN, Martin D, Millar D, Aram JA, Church J, Lodge D. Differences in results from in vivo and in vitro studies on the use-dependency of N-methylaspartate antagonism by MK-801 and other phencyclidine receptor ligands. Eur J Pharmacol. 1988; 145:141–51. [PubMed: 2832187]

Delfs JR, Saroff DM, Nishida Y, Friend J, Geula C. Effects of NMDA and its antagonists on ventral horn cholinergic neurons in organotypic roller tube spinal cord cultures. J Neural Transm. 1997; 104:31–51. [PubMed: 9085191]

Denny MF, Atchison WD. Methylmercury-induced elevations in intrasynaptosomal zinc concentrations, An $^{19}$F-NMR study. J NeurocheM. 1994; 63:383–6. [PubMed: 8207443]

Denny MF, Hare MF, Atchison WD. Methylmercury alters intrasynaptosomal concentrations of endogenous polyvalent cations. Toxicol Appl Pharmacol. 1993; 122:222–32. [PubMed: 7692622]

Edwards JR, Marty MS, Atchison WD. Comparative sensitivity of rat cerebellar neurons to dysregulation of divalent cation homeostasus and cytotoxicity caused by methylmercury. Toxicol Appl Pharmacol. 2005; 208:222–32. [PubMed: 16239166]

Feldman, RS.; Meyer, JS.; Quenzer, LF. Principles of Neuropsychopharmacology. Sinauer Associates, Inc; 1997.

Foster AC, Wong EH. The novel anticonvulsant MK-801 binds to the activated state of the N-methyl-D-aspartate receptor in rat brain. Br J Pharmacol. 1987; 91:403–9. [PubMed: 2886170]

Fox AP, Nowycky MC, Tsien RW. Kinetic and pharmacological properties distinguish three types of calcium currents in chick sensory neurones. J Physiol (Lond). 1978; 394:149–72. [PubMed: 2451016]

Franco JL, Braga HC, Stringari J, Missau FC, Posser T, Mendes BG, Leal RB, Santos AR, Dafre AL, Pizzolatti MG, Farina M. Mercurial-induced hydrogen peroxide generation in mouse brain mitochondria, protective effects of quercetin. Chem Res Toxicol. 2007; 20:1919–26. [PubMed: 17944542]

Fukuyama S, Matsunaga Y, Zhanghui W, Noda N, Asai Y, Moriwaki A, Matsumoto T, Nakano T, Matsumoto K, Nakanishi Y, Inoue HA. Zinc Chelator TPEN attenuates airway hyperresponsiveness and airway inflammation in mice in vivo. Allergol Int. 2011 Feb 25. [Epub ahead of print].

Grosskreutz J, Van Den Bosch L, Keller BU. Calcium dysregulation in amyotrophic lateral sclerosis. Cell Calcium. 2010 Feb; 47(2):165–74. Epub 2010 Jan 29. Review. [PubMed: 20116097]

Hare MF, Atchison WD. Methylmercury mobilizes $Ca^{2+}$ from intracellular stores sensitive to inositol 1,4,5-trisphosphate in NG108-15 cells. J Pharmacol Exp Ther. 1995a; 272:1016–23. [PubMed: 7891311]

Hare MF, Atchison WD. Nifedipine and tetrodotoxin delay the onset of methylmercury- induced increases in $[Ca^{2+}]_i$ in NG108 -15 cells. Toxicol Appl Pharmacol. 1995b; 135:299–307. [PubMed: 8545840]

Hare MF, McGinnis KM, Atchison WD. Methylmercury increases intracellular concentrations of $Ca^{2+}$ and heavy metals in NG108-15 cells. J Pharmacol Exp Ther. 1993; 266:1626–35. [PubMed: 8371160]

Hille B. Ionic channels in nerve membranes. Prog Biophys Mol Biol. 1970; 21:1–32. [PubMed: 4913288]

Houser CR, Barber RP, Crawford GD, Matthews DA, Phelps PE, Salvaterra PM, Vaughn JE. Species-specific second antibodies reduce spurious staining in immunocytochemistry. J Histochem Cytochem. 1984; 32:395–402. [PubMed: 6368679]

Hughes WL. A physiochemical rationale for the biological activity of mercury and its compounds. Ann NY Acad Sci. 1957; 65:454–60. [PubMed: 13411943]

Hunter D, Russell DS. Focal cerebral and cerebellar atrophy in a human subject due to organic mercury compounds. J Neurol Neurosurg Psychiatry. 1954; 17:235–41. [PubMed: 13212411]

Johnson FO, Atchison WD. The role of environmental mercury, lead and pesticide exposure in development of amyotrophic lateral sclerosis. Neurotoxicology. 2009; 30:761–5. [PubMed: 19632272]

Johnson FO, Yuan Y, Hajela RK, Parsell DM, Chitrakar A, Atchison WD. Exposure to an environmental neurotoxicant hastens the onset of ALS phenotype in hSOD1G93A mice: glutamate-mediated excitotoxicity. J Pharmacol Exp Ther. 2011 May 17. [Epub ahead of print].

Kamel F, Umbach DM, Stallone L, Richards M, Hu H, Sandler DP. Association of lead exposure with survival in Amyotrophic Lateral Sclerosis (ALS). Neurology. 2008; 116(7):943–947.

Kamel F, Umbach DM, Munsat TL, Shefner JM, Hu H, Sandler DP. Lead exposure and amyotrophic lateral sclerosis. Epidemiology. 2002; 13:311–19. [PubMed: 11964933]

Komulainen H, Bondy SC. Increased free intrasynaptosomal $Ca^{2+}$ by neurotoxic organometals, distinctive mechanisms. Toxicol Appl Pharmacol. 1987; 88:77–86. [PubMed: 2436355]

Lei SZ, Zhang D, Abele AE, Lipton SA. Blockade of NMDA receptor-mediated mobilization of intracellular $Ca^{2+}$ prevents neurotoxicity. Brain Res. 1992; 598:196–202. [PubMed: 1486480]

Levesque PC, Hare MF, Atchison WD. Inhibition of mitochondrial Ca2+ release diminishes the effectiveness of methyl mercury to release acetylcholine from synaptosomes. Toxicol Appl Pharmacol. 1992; 115:11–20. [PubMed: 1378659]

Leyshon-Sørland K, Jasani B, Morgan AJ. The localization of mercury and metallothionein in the cerebellum of rats experimentally exposed to methylmercury. Histochem J. 1994; 26:161–9. [PubMed: 8150662]

Limke TL, Atchison WD. Acute exposure to methylmercury opens the mitochondrial permeability transition pore in rat cerebellar granule cells. Toxicol Appl Pharmacol. 2002; 178:52–61. [PubMed: 11781080]

Limke TL, Otero-Montañez JK, Atchison WD. Evidence for interactions between intracellular calcium stores during methylmercury-induced intracellular calcium dysregulation in rat cerebellar granule neurons. J Pharmacol Exp Ther. 2003; 304:949–58. [PubMed: 12604669]

Limke TL, Heidemann SR, Atchison WD. Disruption of intraneuronal divalent cation regulation by methylmercury: are specific targets involved in altered neuronal development and cytotoxicity in methylmercury poisoning? Neurotoxicology. 2004; 25:741–60. [PubMed: 15288506]

Marty MS, Atchison WD. Pathways mediating $Ca^{2+}$ entry in rat cerebellar granule cells following in vitro exposure to methyl mercury. Toxicol Appl Pharmacol. 1997; 147:319–30. [PubMed: 9439727]

Marty MS, Atchison WD. Elevations of intracellular $Ca^{2+}$ contribute to decreased viability of cerebellar granule cells following acute exposure to methylmercury. Toxicol. Appl Pharmacol. 1998; 150:98–105.

Mitchell JD. Heavy metals and trace elements in amyotrophic lateral sclerosis. Neurol Clin. 1987; 5:43–60. [PubMed: 3550416]

Moore JW, Blaustein MP, Anderson NC, Narahashi T. Basis of tetrodotoxin's selectivity in blockage of squid axons. J Gen Physiol. 1967; 50:1401–11. [PubMed: 6033592]

Mori N, Yasutake A, Hirayama K. Comparative study of activities in reactive oxygen species production/defense system in mitochondria of rat brain and liver, and their susceptibility to methylmercury toxicity. Arch Toxicol. 2007; 81:769–76. [PubMed: 17464500]

Muller D, Joly M, Lynch G. Contributions of quisqualate and NMDA receptors to the induction and expression of LTP. Science. 1988; 242:1694–7. [PubMed: 2904701]

Nagashima K. A review of experimental methylmercury toxicity in rats, neuropathology and evidence for apoptosis. Toxicol Pathol. 1997; 25:624–31. [PubMed: 9437808]

Nowak L, Bregestovski P, Ascher P, Herbet A, Prochiantz A. Magnesium gates glutamate-activated channels in mouse central neurones. Nature (Lond). 1984; 307:462–5. [PubMed: 6320006]

Oh SS, Kim EA, Lee SW, Kim MK, Kang SK. A case of amyotrophic lateral sclerosis in electronic parts manufacturing worker exposed to lead. Neurotoxicology. 2007; 28:324–7. [PubMed: 17374398]

Pamphlett R, Slater M, Thomas S. Oxidative damage to nucleic acids in motor neurons containing mercury. J Neurol Sci. 1998; 159:121–6. [PubMed: 9741394]

Praline J. ALS and mercury intoxication: a relationship? Clin Neurol Neurosurg. 2007; 109:880–3. [PubMed: 17719172]

Rabenstein DL. The chemistry of methylmercury toxicology. J Chem Educ. 1978; 55:292–6.

Randall A, Tsien RW. Pharmacological dissection of multiple types of $Ca^{2+}$ channel currents in rat cerebellar granule neurons. J Neurosci. 1995; 15:2995–3012. [PubMed: 7722641]

Schramm M, Eimerl S, Costa E. Serum and depolarizing agents cause acute neurotoxicity in cultured cerebellar granule cells, role of glutamate receptor responsive to N-methyl-D-aspartate. Proc Natl Acad Sci. 1990; 87:1193–7. [PubMed: 2153974]

Schulz M, Raju T, Ralston G, Bennett MR. A retinal ganglion cell neurotrophic factor purified from the superior colliculus. J Neurochem. 1990; 55:832–41. [PubMed: 2200848]

Shafer TJ, Atchison WD. Effects of methylmercury on perineurial $Na^+$ and $Ca^{2+}$-dependent potentials at neuromuscular junctions of the mouse. Brain Res. 1992; 595:215–9. [PubMed: 1334771]

Shanker G, Aschner M. Methylmercury-induced reactive oxygen species formation in neonatal cerebral astrocytic cultures is attenuated by antioxidants. Brain Res Mol Brain Res. 2003; 110:85–91. [PubMed: 12573536]

Shrivastav BB, Brodwick BS, Narahashi T. Methylmercury: effects on electrical properties of squid axon membranes. Life Sci. 1976; 18:1077–81. [PubMed: 933697]

Su M, Wakabayashi K, Kakita A, Ikuta F, Takahashi H. Selective involvement of large motor neurons in the spinal cord of rats treated with methylmercury. J Neurol Sci. 1998; 156:12–17. [PubMed: 9559981]

Temkin R, Lowe D, Jensen P, Hatt H, Smith DO. Expression of glutamate receptor subunits in alpha-motoneurons. Brain Res Mol Brain Res. 1997; 52:38–45. [PubMed: 9450675]

Traxinger DL, Atchison WD. Reversal of methylmercury-induced block of nerve-evoked release of acetylcholine at the neuromuscular junction. Toxicol Appl Pharmacol. 1987; 90:23–33. [PubMed: 3629589]

Urushitani M, Nakamizo T, Inoue R, Sawada H, Kihara T, Honda K, Akaike A, Shimohama S. N-methyl-D-aspartate receptor-mediated mitochondrial $Ca^{2+}$ overload in acute excitotoxic motor neuron death, a mechanism distinct from chronic neurotoxicity after $Ca^{2+}$ influx. J Neurosci Res. 2001; 63:377–87. [PubMed: 11223912]

Usuki F, Yasutake A, Umehara F, Tokunaga H, Matsumoto M, Eto K, Ishiura S, Higuchi I. In vivo protection of a water-soluble derivative of vitamin E. Trolox, against methylmercury-intoxication in the rat. Neurosci Lett. 2001; 304:199–203. [PubMed: 11343836]

Van den Bosch L. The causes and mechanism of selective motor neuron death in amyotrophic lateral sclerosis. Verh K Acad Geneeskd Belg. 2006; 68(4):249–69. Review. Dutch. [PubMed: 17214440]

Van Den Bosch L. Genetic rodent models of amyotrophic lateral sclerosis. J Biomed Biotechnol 2011. 2011:348765. Epub 2011 Jan 2. Review.

Vanacore N, Corsi L, Fabrizio E, Bonifati V, Meco G. Relationship between exposure to environmental toxins and motor neuron disease, a case report. Med Lav. 1995; 86:522–33. [PubMed: 8815363]

Westenbroek RE, Sakurai T, Elliott EM, Hell JW, Starr TV, Snutch TP, Catterall WA. Immunochemical identification and subcellular distribution of the $\alpha_{1A}$ subunits of brain calcium channels. J Neurosci. 1995; 15:6403–18. [PubMed: 7472404]

Wong V, Arriaga R, Ip NY, Lindsay RM. The neurotrophins BDNF, NT-3 and NT-4/5, but not NGF, up-regulate the cholinergic phenotype of developing motor neurons. Eur J Neurosci. 1993; 5:466–74. [PubMed: 7505167]

Yuan Y, Atchison WD. Methylmercury-induced increase of intracellular $Ca^{2+}$ increases spontaneous synaptic current frequency in rat cerebellar slices. Mol Pharmacol. 2007; 71:1109–21. [PubMed: 17244699]
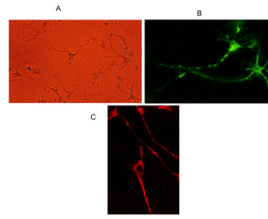
**Figure 1.**
Six day old primary cultures of mouse spinal motor neurons. Fig 1A - Brightfield image. Fig 1B: Motor neurons immunolabelled with choline acetyltransferase (ChAT) -a specific marker for motor neurons. Note the large multipolar neurons with long axons. Fig 1C: Motor neurons immunolabeled with SMI-32 a specific marker for non-phosphorylated 200 kD Neurofilament Heavy.
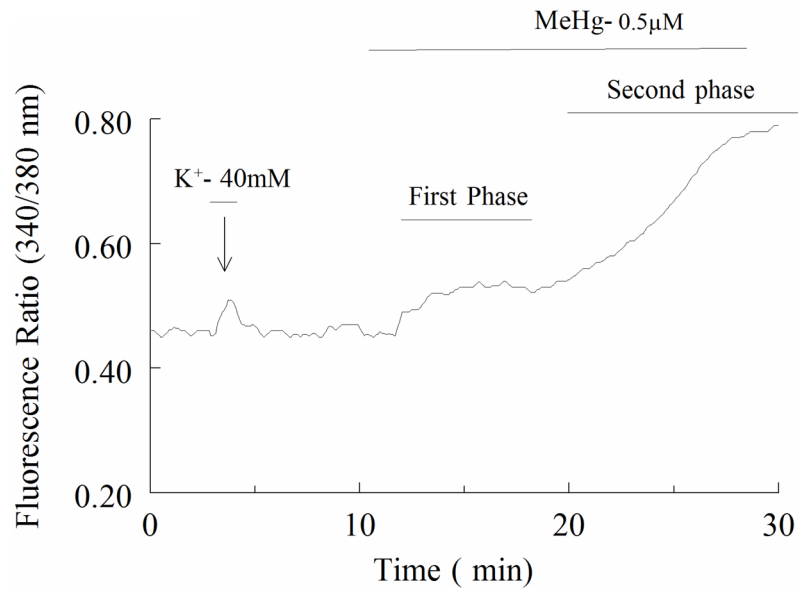
**Figure 2.**
A representative tracing showing the time course of changes in fura-2 fluorescence ratio for spinal motor neurons exposed to 0.5 μM MeHg. The cell was initially exposed to 40 mM $K^+$ for 1 min to verify cell viability and $Ca^{2+}$ buffering capacity. MeHg was added where indicated; the biphasic nature of the MeHg response is indicated. The first phase, is small, whereas the magnitude of fluorescence ratio increase during the second phase is markedly increased.
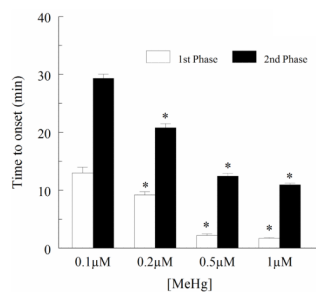
**Figure 3.**
Effect of MeHg (0.1–1µM) on the time to onset of both first phase and second phase increases in fura-2 fluorescence ratio. The time to onset increase is inversely related to the concentration of MeHg used. The asterisk (*) reflects a significant difference between the response at 0.1 µM MeHg and higher concentrations (p < 0.05). This demonstrates a correlation between the [MeHg] and time to onset of the response for each phase. Values are the mean ± SEM of 5 separate cultures.
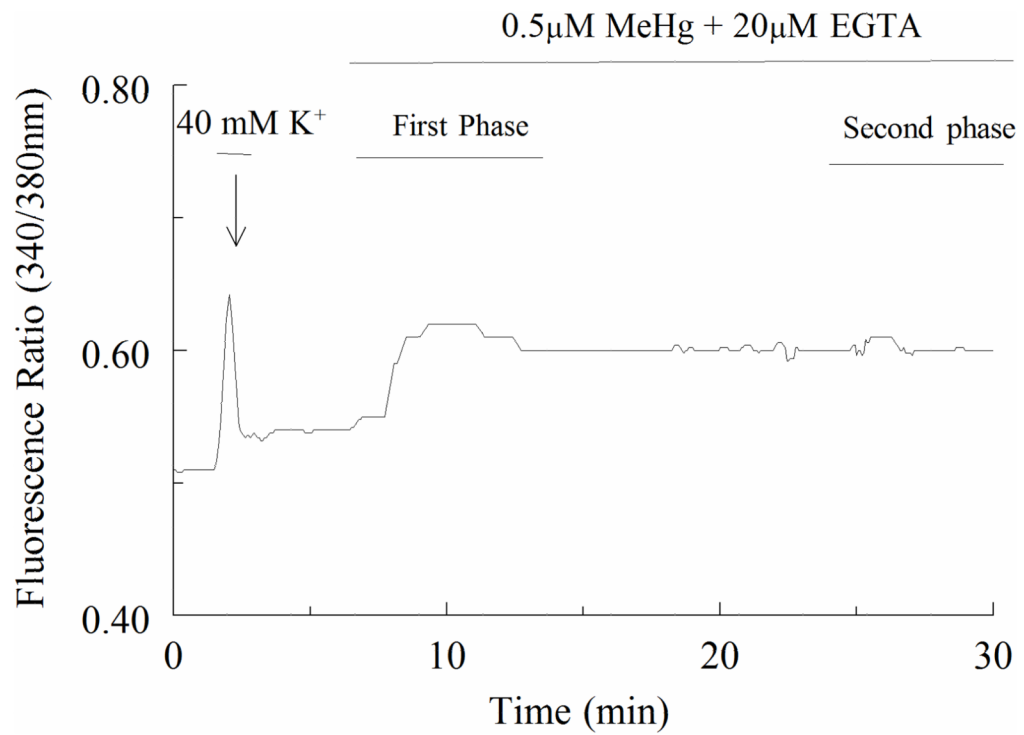
**Figure 4.**
Representative tracing showing changes in fura-2 fluorescence intensity for spinal motor neurons exposed to 0.5μM MeHg with 20μM EGTA. The cell was initially exposed to 40 mM $K^+$ for 1 min (arrow) as in Figure 2. MeHg + EGTA was added where indicated. The biphasic nature of the MeHg response is now modified; the first phase remains, while the second phase increase of fura-2 is absent indicating that it requires $Ca^{2+}$.
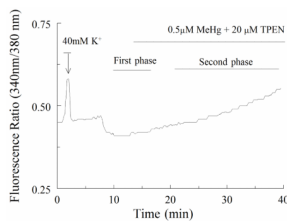
**Figure 5.**
A representative tracing illustrating that the MeHg exposure induced first phase is not fully dependent on $Ca^{2+}$. There are contributions from other cations such as $Zn^{2+}$, $Fe^{2+}$ or $Mn^{2+}$. MeHg plus the non-$Ca^{2+}$ divalent cation chelator TPEN (20μM) were added where indicated. Note the apparent absence of a first phase, but presence of an increase in fluorescence ratios during the second phase, indicating that TPEN chelates the non $Ca^{2+}$ cations and the first phase can be caused by non-$Ca^{2+}$ cations as well (Fukuyama et al., 2011; Aizenman et al; 2010).
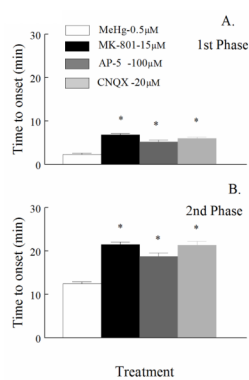
**Figure 6.**
Effect of NMDA and non-NMD receptor blockers on the time-to-onset of fluorescence changes induced by MeHg. Spinal motor neurons were exposed 0.5 μM MeHg (white) alone or in combinations with 15μM MK-801 (black), 100 μM AP-5 (dark gray), or 100 μM CNQX (light gray); all inhibitors were added 7 min prior to MeHg. There is a significant (*p*<0.05) difference in time-to-onset of both the first and the second phase in the presence of inhibitors compared to MeHg alone. Values are the mean ± SEM of 5 separate cultures.
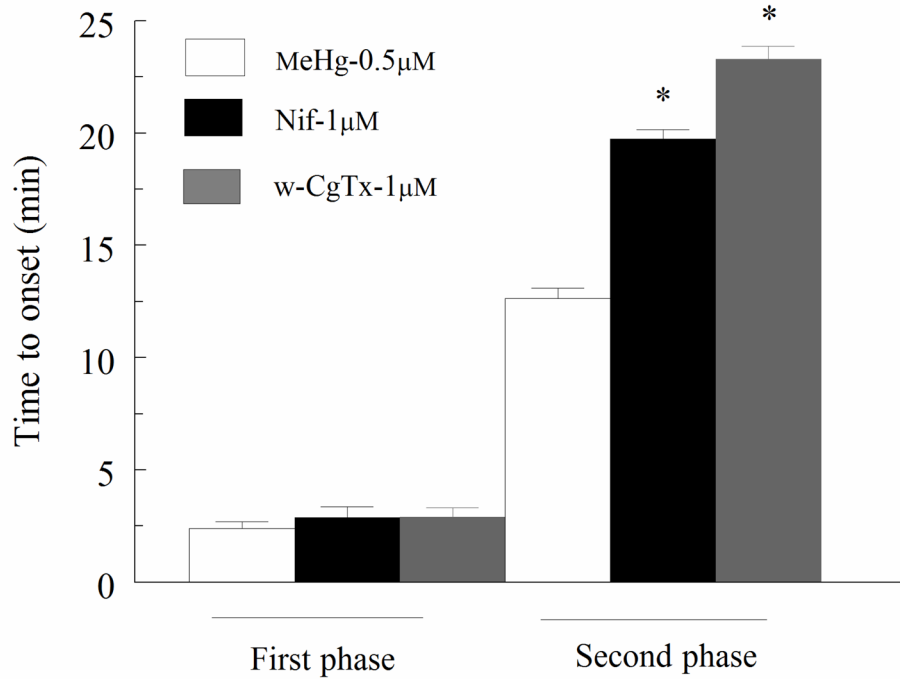
**Figure 7.**
Effect of nifedipine (L-type) or ω-CTx-GVIA (N-type) $Ca^{2+}$ channel on time-to-onset of fluorescence changes induced by MeHg. Spinal motor neuron were 0.5 μM MeHg alone (white bars) or together with 1μM nifedipine (medium gray) or 1μM ω-CTx-GVIA (dark gray bars). All inhibitors were added 7 min prior to MeHg. No change occurred in the time to onset of the first phase but there is a significant $p<0.05$) difference in time-to onset of the second phase in the presence of these channel inhibitors compared to MeHg alone ($n = 5$). Values are the mean ± SEM of 5 separate cultures.
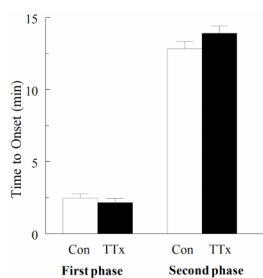
**Figure 8.**
Effect of TTX (1µM) a $Na^+$ channel blocker on MeHg-induced (0.5 µM) changes in fura-2 fluorescence. TTX, did not significantly ($p > 0.05$) alter the time to onset of either phase. Therefore $Na^+$ channels did not contribute to the effect of MeHg on $[Ca^{2+}]_i$ in spinal motor neurons ($n = 5$).

The effect of TPEN/EGTA on the response of spinal motor neurons to acutely applied MeHg

| Treatment | Phase | cell 1 | cell 2 | cell 3 | cell 4 | cell 5 | cell 6 |
|---|---|---|---|---|---|---|---|
| 0.5μM MeHg | I | + | + | + | + | + | + |
|  | II | + | + | + | + | + | + |
| 0.5μM MeHg +20μM TPEN | I | – | – | – | – | – | – |
|  | II | + | + | + | + | + | + |
| 0.5μM MeHg | I | + | + | + | + | + | + |
|  | II | + | + | + | + | + | + |
| 0.5μM MeHg + 20μM EGTA | I | + | + | + | + | + | + |
|  | II | – | – | – | – | – | – |

MeHg alone or MeHg + 20μM TPEN or 20μM EGTA was applied to six spinal motor neurons for each experiment (*n*=6). Presence of the two kinetically distinct phases of increased fluorescence was examined. There is a statistically significant difference (p>0.05) in the presence and absence of the phase when the cells were exposed to MeHg alone and MeHg with TPEN/EGTA.

Note: "+" indicates the phase is present, "—" indicates that it is absent.